Photoreactions of the Triruthenium Cluster $Ru_3(CO)_{12}$ and Substituted Analogues[1,2]

Marc F. Desrosiers, David A. Wink, Ray Trautman, Alan E. Friedman, and Peter C. Ford*

Contribution from the Department of Chemistry, University of California, Santa Barbara, California 93106. *Received September 9, 1985*

Abstract: Reported is a comprehensive investigation of the medium, ligand, and wavelength effects on the quantum yields and flash photolysis kinetics for the photofragmentation and photosubstitution reactions of the trinuclear ruthenium cluster $Ru_3(CO)_{12}$. Also described are some related studies of the substituted clusters $Ru_3(CO)_{12-n}L_n$ (L = $P(OCH_3)_3$, PPh_3, $P(p\text{-tolyl})_3$, or $P(O(o\text{-tolyl}))_3$). These results are interpreted in terms of the following model for $Ru_3(CO)_{12}$ photochemistry. Photofragmentation (e.g., $Ru_3(CO)_{12} + 3L \rightarrow 3Ru(CO)_4L$) occurs predominantly from the lowest energy excited state and proceeds via an intermediate (I) isomeric to $Ru_3(CO)_{12}$ but not a diradical. I is proposed to have one coordinatively unsaturated ruthenium center trapable by a two-electron donor, i.e., L, to give a second intermediate $Ru_3(CO)_{12}L$ which is the precursor to the photofragmentation products. Kinetic flash photolysis observations demonstrate that the lifetime of the latter intermediate is markedly dependent on the nature of L. Photosubstitution reactions (e.g., $Ru_3(CO)_{12} + L \rightarrow Ru_3(CO)_{11}L + CO$) are proposed to occur largely from higher energy excited states via CO dissociation to give the unsaturated intermediate $Ru_3(CO)_{11}$, and flash photolysis studies establish the reactivity of this species with various L to follow the order $CO > P(OCH_3)_3 > PPh_3$.

There have been a number of reports of the photochemical reactivity of metal carbonyl clusters, and such reactions have proved useful for the synthesis both of new metal clusters and of certain mononuclear metal carbonyl derivatives[3-14] and for the generation of catalysts for organic transformations.[15-19] However, unlike the mono- and dinuclear metal carbonyls which have been (and continue to be) intensively investigated,[20] the cluster compounds have been the subject of relatively few quantitative photochemical studies.[2,9,21-29] Described here is such a quantitative investigation of the chemistry resulting from both continuous and flash photolysis of the triangular metal carbonyl cluster $Ru_3(CO)_{12}$, which is one of the simplest, thermally stable metal carbonyl clusters and can serve as a prototype for the photoreactivity of such species.

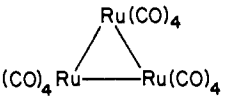

Of particular interest regarding clusters are the mechanisms of reactions leading to the cleavage of metal–metal bonds, for example, the photofragmentation of $Ru_3(CO)_{12}$ first described by Johnson, Lewis, and Twigg.[5]

$$Ru_3(CO)_{12} + 3CO \xrightarrow{h\nu} 3Ru(CO)_5 \qquad (1)$$

Dinuclear complexes have been shown to undergo fragmentation to mononuclear species by both homolytic cleavage of the metal–metal bond, e.g.,[30,31]

$$[(\eta^5\text{-}C_5H_5)W(CO)_3]_2 \xrightarrow{h\nu} 2(\eta^5\text{-}C_5H_5)W(CO)_3\cdot \qquad (2)$$

and by pathways proposed to involve heterolytic bond cleavage,[32] although the former appears to the more prevalent mechanism.[33] The reason for this behavior has been attributed to the nature of the dominant lower energy absorption bands of molecules such as the tungsten dimer (above) which have been assigned as $\sigma_{MM} \rightarrow \sigma_{MM}^*$ or $d \rightarrow \sigma_{MM}^*$ transitions leading to states having greatly weakened M–M bonds.[30] For cluster species, the lower energy electronic transitions generally involve excited states for which metal–metal bonding is diminished. Such states are delocalized over several metal centers[34,35] and this delocalization may qual-

(1) (a) Taken largely from the Ph.D. dissertation of M.E.D. (UCSB, 1983) and in part from the Ph.D. dissertation of D.A.W. (UCSB, 1985). (b) Reported in part at the 183rd National Meeting of the American Chemical Society, Las Vegas, NV, April 1982; American Chemical Society: Washington, D.C., 1982; INOR 92, and at the XXIII International Conference on Coordination Chemistry, Boulder, CO, August 1984.

(2) Preliminary accounts of this work were the following: (a) Desrosiers, M. F.; Ford, P. C. *Organometallics* **1982**, *1*, 1715–1716. (b) Desrosiers, M. F.; Wink, D. A.; Ford, P. C. *Inorg. Chem.* **1985**, *24*, 1–2.

(3) Evans, G. O.; Sheline, R. K. *J. Inorg. Chem.* **1968**, *30*, 2862–2863.

(4) Cullen, W. R.; Harbourne, D. A. *Inorg. Chem.* **1970**, *9*, 1839–1843.

(5) Johnson, B. F. G.; Lewis, J.; Twigg, M. V. *J. Organomet. Chem.* **1974**, *67*, C75–76.

(6) Johnson, B. F. G.; Lewis, J.; Twigg, M. V. *J. Chem. Soc., Dalton Trans.* **1975**, 1876–1879.

(7) Burkhardt, E. W.; Geoffroy, G. L. *J. Organomet. Chem.* **1980**, *198*, 179–188.

(8) Grevels, F.-W.; Reuvers, J. G. A.; Takats, J. *Angew. Chem., Int. Ed. Engl.* **1981**, *20*, 452–460.

(9) Grevels, F.-W.; Reuvers, J. G. A.; Takats, J. *J. Am. Chem. Soc.* **1981**, *103*, 4069–4073.

(10) Doi, Y.; Yano, K. *Inorg. Chem. Acta* **1983**, *76*, L71–L73.

(11) Leopold, D. G.; Vaida, V. *J. Am. Chem. Soc.* **1983**, *105*, 6809–6811.

(12) Burke, M. R.; Takats, J.; Grevels, F.-W.; Reuvers, J. G. A. *J. Am. Chem. Soc.* **1983**, *105*, 4092–4093.

(13) Liu, D. K.; Wrighton, M. S.; McKay, D. R.; Maciel, G. E. *Inorg. Chem.* **1981**, *23*, 212–220.

(14) Benison, J. G.; Wrighton, M. S. *Inorg. Chem.* **1984**, *23*, 512–515.

(15) Bamford, C. H.; Mahmud, M. V. *J. Chem. Soc., Chem. Commun.* **1972**, 762–763.

(16) Austin, R. G.; Paonessa, R. S.; Giordano, P. J.; Wrighton, M. S. *Adv. Chem. Ser.* **1978**, *168*, 189–214.

(17) (a) Graff, J. L.; Sanner, R. D.; Wrighton, M. S. *J. Am. Chem. Soc.* **1979**, *101*, 273–275. (b) Graff, J. L.; Wrighton, M. S. *J. Am. Chem. Soc.* **1980**, *102*, 2123–2125.

(18) Graff, J. L.; Sanner, R. D.; Wrighton, M. S. *Organometallics* **1982**, *1*, 837–842.

(19) Doi, Y.; Tamura, S.; Koshizuki, K. *J. Mol. Catal.* **1983**, *19*, 213–222.

(20) Geoffroy, G. L.; Wrighton, M. S. "Organometallic Photochemistry"; Academic Press: New York, 1979.

(21) Bock, C. R.; Wrighton, M. S. *Inorg. Chem.* **1977**, *16*, 1309–1313.

(22) Geoffroy, G. L.; Epstein, R. A. *Inorg. Chem.* **1977**, *16*, 2795–2799. Geoffroy, G. L.; Epstein, R. A. *Adv. Chem. Ser.* **1978**, *168*, 132–146.

(23) Epstein, R. A.; Gaffney, T. R.; Geoffroy, G. L.; Gladfelter, W. L.; Henderson, R. S. *J. Am. Chem. Soc.* **1979**, *101*, 3847–3852.

(24) Tyler, D. R.; Altobelli, M.; Gray, H. B. *J. Am. Chem. Soc.* **1980**, *102*, 3022–3024.

(25) Foley, H. C.; Geoffroy, G. L. *J. Am. Chem. Soc.* **1981**, *103*, 7176–7180.

(26) Graff, J. L.; Wrighton, M. S. *J. Am. Chem. Soc.* **1981**, *103*, 2225–2231.

(27) Tyler, D. R.; Gray, H. B. *J. Am. Chem. Soc.* **1981**, *103*, 1683–1686.

(28) Malito, J.; Markiewicz, S.; Poë, A. *Inorg. Chem.* **1982**, *21*, 4335–4338.

(29) Amadelli, R.; Carassiti, V.; Maldotti, A.; Aime, S.; Osella, D.; Milone, L. *Inorg. Chim. Acta* **1984**, *81*, L11–13.

(30) Wrighton, M. S.; Ginley, D. S. *J. Am. Chem. Soc.* **1975**, *97*, 4246–4251.

(31) Laine, R. M.; Ford, P. C. *Inorg. Chem.* **1977**, *16*, 388–391.

(32) Haines, R. J.; Nyholm, R. S.; Stiddard, M. H. B. *J. Chem. Soc. A* **1968**, 43–46.

(33) Sleigman, A. E.; Tyler, D. R. *Inorg. Chem.* **1984**, *23*, 527–529.

(34) Tyler, D. R.; Levenson, R. A.; Gray, H. B. *J. Am. Chem. Soc.* **1978**, *100*, 7888–7893.

(35) (a) Delley, B.; Manning, M. C.; Ellis, D. E.; Berkowitz, J.; Trogler, W. C. *Inorg. Chem.* **1982**, *21*, 2247–2253. (b) Manning, M. C.; Trogler, W. C. *Coord. Chem.* **1981**, *214*, 115–118.

0002-7863/86/1508-1917$01.50/0 © 1986 American Chemical Society

itatively decrease the probability of metal–metal bond cleavage relative to other deactivation channels available to the excited state. Furthermore, the hinging of the two centers representing the termini of a metal–metal bond greatly increases the probability of reformation of this bond if cleaved. Thus, it is not surprising that photofragmentation yields of clusters are generally found to be small.

Our initial interest in the photochemistry of the triruthenium cluster $Ru_3(CO)_{12}$ stemmed from attempts to use the photofragmentation depicted in eq 1 as a route to preparation of the mononuclear species $Ru(CO)_5$ in various solvents.[36] While the original preparation in hydrocarbon solvents proved quite effective, similar photolysis in more polar solvents led such to the formation of insoluble red polymers later shown to have the approximate composition $[Ru(CO)_{3.5}]_n$.[37] These differences prompted the investigation of media effects on the photoreactions of $Ru_3(CO)_{12}$ and some derivatives. In the course of these studies, it was also found that, although lower energy excitation leads almost exclusively to cluster fragmentation, photolysis at shorter wavelengths results in ligand substitution as well (eq 3). Furthermore, flash photolysis experiments demonstrated the existence of intermediates in both photoreactions.

$$Ru_3(CO)_{12} + L \xrightarrow{h\nu} Ru_3(CO)_{11}L + CO \qquad (3)$$

Experimental Section

Materials. The solvents used were reagent grade and were purified as follows. Tetrahydrofuran (THF) was distilled from sodium benzophenone under Ar. Normal octane (Aldrich Gold Label) was first washed with concentrated H_2SO_4 several times and then with water until no longer acidic, dried with $MgSO_4$, and distilled. Cyclohexane (Aldrich Gold Label) was distilled from $LiAlH_4$ under N_2. Di(2-methoxyethyl)ether (diglyme) was distilled from CaH_2. Cyclohexene was distilled neat, and 2-methyltetrahydrofuran (MeTHF) was distilled from Na. The gases CO (CP grade), 25% CO/75% N_2, 10% CO/90% N_2, Ar, and ethylene were purchased from Linde.

The ruthenium complexes $Ru_3(CO)_{12}$,[38] $Ru_3(CO)_{11}L$,[39] $Ru_3(CO)_{10}L_2$,[39] $Ru_3(CO)_9L_3$[39] (L = $P(OCH_3)_3$, PPh_3, or $P(p\text{-tolyl})_3$) and $Ru(CO)_4(P(OCH_3)_3)$[40] were prepared by published procedures.

Instrumentation and Procedures. Electronic and infrared spectra were recorded on Cary 118 and Perkin-Elmer 683 spectrophotometers, respectively. Continuous (CW) photolyses were carried out at irradiation wavelengths (λ_{irr}) 254, 313, 334, 365, and 405 nm by using apparatus and procedures described previously.[41] Light intensities were measured by ferrioxalate actinometry. Deaerated solutions for CW photolysis experiments and dark reaction controls were prepared under Ar, CO, or C_2H_4 and transferred to quartz photolysis cells by using either Zwickel flask[42] or vacuum manifold procedures. Spectral changes (electronic or IR) were recorded to evaluate dark and photoreactions. Quantum yields were calculated from the concentration changes so determined. In all cases, dark reaction controls showed analogous thermal reactions to be much slower than photoprocesses under the experimental conditions.

Solutions for flash photolysis experiments were prepared via vacuum manifold techniques and transferred without exposure to air into 20-cm pathlength quartz cells with concentric outer jackets for filter solutions. Photolysis wavelength selection was accomplished by use of different aqueous solutions in this outer jacket. These, which served as short wavelength cutoff filters, were 0.1 M $NaNO_2$ (λ_{cutoff} = 395 nm), 1.0 M $NaNO_3$ (320 nm), and 0.1 M Na_2SO_3 (254 nm). Special care was taken to ensure purity of solvents for flash experiments and that reaction solutions were completely deaerated. Redistilled solvents were introduced to the greaseless vacuum manifold by syringe then degassed by six consecutive freeze–pump–thaw cycles. The solvents were then distilled from a Na/K amalgam into a previously evacuated flash photolysis cell containing ligand and metal cluster in the correct proportions. Unless otherwise indicated, flash experiments were carried out under argon (1.0 atm) which had been purified by passing consecutively through columns containing BASF catalyst, dried molecular sieve, and CrO/SiO_2. The flash apparatus and procedures have been described previously[43] with the exception that the present apparatus is interfaced through a Biomation 805 transient digitizer to a Hewlett-Packard 86 computer for recording and computation of data.

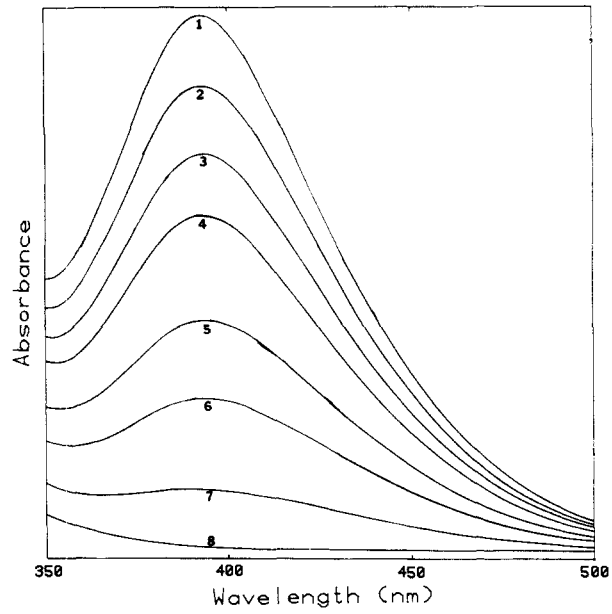

Figure 1. Sequential spectra recorded during the 405-nm photolysis of $Ru_3(CO)_{12}$ plus $P(OCH_3)_3$ (0.012 M) in octane solution. (1 is the initial spectrum.)

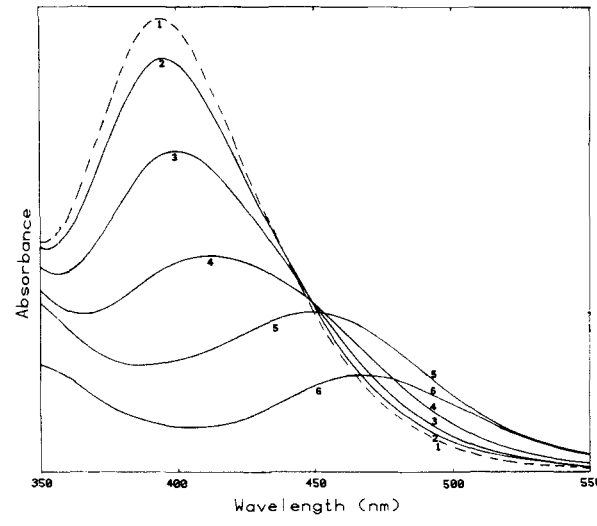

Figure 2. Sequential spectra recorded during the 313-nm photolysis of $Ru_3(CO)_{12}$ plus $P(OCH_3)_3$ (0.012 M) in octane solution. (1 is the initial spectrum.)

Results

The photochemistry of $Ru_3(CO)_{12}$ has been shown to involve two different types of reaction: photofragmentation of the cluster[5] and photolabilization of one or more carbonyls to give substituted trinuclear clusters $Ru_3(CO)_{12-n}L_n$.[2b,4]

The electronic spectrum of $Ru_3(CO)_{12}$ is dominated by an intense absorption band centered at 392 nm ($\epsilon_{max} = 7.7 \times 10^3$ M^{-1} cm^{-1} in cyclohexane solution). Replacement of one or more carbonyls by a phosphine or phosphite ligand leads to a shift of

(36) Yarrow, P.; Ford, P. C. *J. Organomet. Chem.* **1981**, *214*, 115–118.
(37) Trautman, R., unpublished observations in this laboratory.
(38) Eady, C. R.; Jackson, P. F.; Johnson, B. F. G.; Lewis, J.; Malatesta, M. C.; McPartlin, M.; Nelson, W. J. H. *J. Chem. Soc. Dalton Trans.* **1980**, 383–392.
(39) (a) Bruce, M. I.; Kehoe, D. C.; Matisons, J. G.; Nicholson, B. K.; Rieger, P. H.; Williams, M. L. *J. Chem. Soc., Chem. Commun.* **1982**, 442–444. (b) Bruce, M. I.; Matisons, J. G.; Nicholson, B. K. *J. Organomet. Chem.* **1983**, *247*, 321–344.
(40) Cobbeldick, R. E.; Einstein, F. W. B.; Pomeroy, R. K.; Speich, E. R. *J. Organomet. Chem.* **1980**, *195*, 77–88.
(41) (a) Hintze, R. E.; Ford, P. C. *J. Am. Chem. Soc.* **1975**, *97*, 2664–2671. (b) Matsubara, T.; Ford, P. C. *Inorg. Chem.* **1978**, *17*, 1747–1752.
(42) Kuehn, C. G.; Taube, H. *J. Am. Chem. Soc.* **1976**, *98*, 689–702.
(43) Durante, V. A.; Ford, P. C. *Inorg. Chem.* **1979**, *18*, 588–593.

Table I. Photofragmentation Quantum Yields for the 405-nm Photolysis of $Ru_3(CO)_{12}$ in Different Solutions (25 °C)

solution	conditions	[CO][a]	product[b]	$10^3 \times \phi_f$[c]
octane	*d*	0.012	$Ru(CO)_5$	28.0 ± 4
octane	P_{CO} = 0.00[e]	0.00	$Ru(CO)_5$	<0.1
octane, 0.5 M THF	*d*	0.012	$Ru(CO)_5$	1.7 ± 0.0
octane, 1.0 M cyclohexene	P_{CO} = 0.0	0.00	not determined	1.6 ± 0.2
cyclohexane	P_{CO} = 1.0	0.0092	$Ru(CO)_5$	18.0 ± 1
cyclohexane	P_{CO} = 0.25[f]	0.0023	not determined	4.4 ± 1.3
cyclohexane	P_{CO} = 0.10[f]	0.00092	not determined	2.2 ± 0.1
THF	*d*	0.0084	$Ru(CO)_5$	3.5 ± 0.7
diglyme	*d*	0.0053	$Ru(CO)_5$	0.7 ± 0.1
octane, 1.0 M CCl_4	*d*	0.012	$Ru_z(CO)_xCl_y$[g]	24.0 ± 4
octane, 1.0 M CCl_4	P_{CO} = 0.0[e]	0.0	$Ru_z(CO)_xCl_y$[g]	0.2
octane, 1 M CCl_4, 1 M THF	*d*	0.012	not determined	1.0 ± 0.1
CCl_4	*d*	0.0089	$Ru_z(CO)_xCl_y$[g]	13.0 ± 3
CCl_4	P_{CO} = 0.0[e]	0.000	$Ru_z(CO)_xCl_y$[g]	0.7 ± 0.1

[a] CO concentrations (in mol/L) were estimated from literature data as follows: Octane, CO solubility assumed to be the same as *n*-heptane (0.012 mol/l atm). Seidell, A.; Linke, W. "Solubilities of Inorganic and Metal Organic Compounds", 4th ed.; D. van Nostrand Co.: Princeton, NJ, p 456. Cyclohexane (0.0092 mol/L atm), Wilhelm, E.; Battino, R. *Chem. Rev.* **1973**, *73*, 1. THF, solubility (0.0084 mol/L atm) estimated from the methods of solution theory as described in the "Encyclopedia of Chemical Technology", 3rd ed.; Wiley: New York, 1978; Vol. 21, p 377. Diglyme (0.0053 mol/l atm), Hildebrand, J.; M. S. Dissertation in Chemical Engineering, University of California, Santa Barbara, 1979 (note: the value 0.006 mol/L atm reported in ref 2a was slightly in error). Carbon tetrachloride (0.0089 mol/l atm), Seidell, A.; Linke, W., as cited above. [b] Products identified from IR spectra. [c] In moles per einstein. [d] P_{CO} = 1.0 atm except where noted, 25 °C. [e] P_{Ar} = 1.0 atm. [f] Total pressure = 1.0 atm, the balance being N_2. [g] See text.

this band to progressively longer wavelengths depending on the nature of the ligand and on the extent of substitution. Given that the mononuclear complexes $Ru(CO)_{5-n}L_n$ do not absorb appreciably in the visible region, photofragmentation of $Ru_3(CO)_{12}$ is indicated by a decrease in the 392-nm band intensity without a shift in the λ_{max} while photosubstitution by L is indicated by shifts in this band to longer wavelengths. For the systems studied quantitatively here, photolysis of $Ru_3(CO)_{12}$ at 405 nm in the presence of a ligand such as $P(OCH_3)_3$ gave spectral changes consistent with photofragmentation only, (e.g., Figure 1), while photolysis at shorter wavelengths gave spectral shifts indicative of the formation of substituted clusters (e.g., Figure 2).

I. Photoreactions of $Ru_3(CO)_{12}$ with CO. Solvent Effects. Photolysis (λ_{irr} 405 nm) of $Ru_3(CO)_{12}$ in octane under CO led to simple bleaching of the 392-nm band. According to the infrared spectrum, the resulting colorless solution contained $Ru(CO)_5$ as the sole metal carbonyl product (eq 1) in agreement with previous reports.[5,36] The quantum yield for photofragmentation (ϕ_f), determined spectrally from disappearance of the 392 nm band, was 0.028 mol/einstein for solutions under CO (P_{CO} 1.0 atm). For solutions prepared without CO (under an Ar atmosphere), fragmentation yields were several orders of magnitude smaller (Table I). Prolonged photolysis (λ_{irr} 405 nm) of the latter solutions led to the formation of small amounts of $Ru(CO)_5$ identified from the ν_{CO} bands of this species at 2040 and 2001 cm^{-1}. No other products were observed.

When 405-nm photolysis of $Ru_3(CO)_{12}$ was carried out in cyclohexane under CO (1.0 atm), $Ru(CO)_5$ was again the product with a ϕ_f about 30% smaller than in octane. The ϕ_f values were markedly dependent on the partial pressure of CO (Table I). In CO equilibrated THF, CW photolysis of dilute ($<10^{-4}$ M) $Ru_3(CO)_{12}$ again gave $Ru(CO)_5$ as the sole product; however, more concentrated solutions gave an insoluble red polymer (approximate composition $[Ru(CO)_{3.5}]_n$ according to elemental analysis)[37] upon prolonged photolysis. The formation of polymer was suppressed somewhat if the photolysis cell was attached to a reservoir with a large excess of CO. The ϕ_f values for the dilute solutions in THF were found to be about an order of magnitude smaller than in octane (Table I). Lastly, 405-nm photolysis of dilute $Ru_3(CO)_{12}$ ($<10^{-4}$ M) solutions in diglyme under CO (1 atm) also gave $Ru(CO)_5$ as the sole product, but ϕ_f in this case was even lower than in THF (Table I). Other workers[28] have also shown that ϕ_f is solvent dependent following the order isooctane (0.044 mol/einstein) > cyclohexane (0.026) ≫ benzene (0.0013) for 366-nm CW irradiation under 1.0 atm CO.

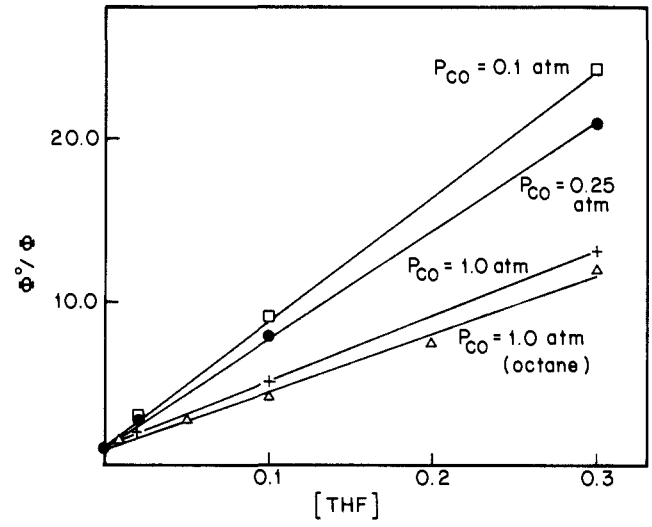

Figure 3. Stern–Volmer type plots for THF quenching of the photofragmentation of $Ru_3(CO)_{12}$ in octane and in cyclohexane under different P_{CO}.

Quenching Studies. In order to evaluate whether the solvent effects represent differences in bulk properties or in microscopic chemical properties, the photofragmentation of $Ru_3(CO)_{12}$ under CO was investigated in octane (λ_{irr} 405 nm) with various concentrations of these and other cosolvents added. The result was significant quenching of the photofragmentation pathway by even relatively small concentrations of certain materials. For example, ϕ_f in a 0.5 M solution of THF in octane was 1.7×10^{-3}, more than an order of magnitude smaller than in octane and, surprisingly, about half the value found in THF itself (Table I). Again, $Ru(CO)_5$ was demonstrated to be the sole metal carbonyl photoproduct. Furthermore, the quantitative behavior of THF as a photoreaction quencher in octane was demonstrated by a linear Stern–Volmer type plot[44] (ϕ_f^0/ϕ_f vs. [THF]) which gave a slope (K_{SV}) of 34 ± 1 M^{-1} (Figure 3). Linear Stern–Volmer plots with the respective K_{SV} values 26 ± 1 and 16 ± 1 M^{-1} were also obtained for the ϕ_f values measured when diglyme or cyclohexene was added to octane solutions of $Ru_3(CO)_{12}$. Similar plots of ϕ_f^0/ϕ_f vs. [THF] were found to be linear in cyclohexane solution with the slopes dependent on the composition of the gas with which the solution was equilibrated. The measured K_{SV} value under 100% CO (1.0 atm) was 40.6 ± 0.5 M^{-1}, close to that measured analogously in octane, but the values measured under 25% CO/75% N_2 and 10% CO/90% N_2 were 66 ± 1 and 83 ± 1 M^{-1}, respectively (Figure 3).

The potential quenching by other donors was examined further by measuring the $Ru_3(CO)_{12}$ photofragmentation yields (λ_{irr} 405 nm) at a single concentration of that species in octane under CO (1.0 atm). Under these conditions, the ϕ_f values were smaller in the presence of added benzene, 2-methyltetrahydrofuran, pyridine, or propionitrile relative to neat octane solutions. In each case the final photoproduct was identified as $Ru(CO)_5$. The resulting ϕ_f's are listed in Table II along with K_{SV}'s estimated from assumed adherence to Stern–Volmer kinetic behavior (i.e., $\phi_f^0/\phi_f = 1 + K_{SV}[Q]$, where [Q] is the concentration of the added quencher). Given that octane solutions of $Ru_3(CO)_{12}$ with added pyridine, cyclohexene, or propionitrile underwent some photofragmentation

(44) Turro, N. J. "Modern Molecular Photochemistry"; Benjamin/Cummings Publishing Co.: Menlo Park, CA, 1978; pp 245–248.

Table II. Fragmentation Quantum Yields for 405-nm CW Photolysis of $Ru_3(CO)_{12}$ in Octane Solution in the Presence of Added Quenchers[a]

quencher	[Q]	$10^3\phi_f$[b]	est. K_{sv}[c] (M^{-1})
none		28.0 ± 4	
THF	0.30	2.4 ± 0.1	36 (34)[d]
diglyme	0.30	3.2 ± 0.1	26 (26)[d]
2-MeTHF	0.30	3.5 ± 0.1	23
cyclohexene	0.20	6.5 ± 0.2	17 (16)[d]
benzene	1.0	9.0 ± 0.5	2.1
pyridine	0.30	15.0 ± 1.0	2.9
acetonitrile	0.30	19.0 ± 0.5	1.6

[a] P_{CO} = 1.0 atm ([CO] = 0.012 mol/L), T = 25 °C, λ_{irr} = 405 nm, [Q] in mol/L. [b] In mol per einstein. [c] Estimated from the relationship $\phi_f^\circ/\phi_f = 1 + K_{sv}[Q]$. [d] Determined from Stern–Volmer plots (see Results).

under an argon atmosphere to give species believed to be the mononuclear $Ru(CO)_4L$ complexes, considering these donors as quenchers is not strictly correct. However, no net photofragmentation was noted under Ar when the only donor present was THF, benzene, or 2-methyltetrahydrofuran.

Halocarbon Solvents. The photofragmentation quantum yields for $Ru_3(CO)_{12}$ in neat CCl_4 solutions and in octane solutions containing 1.0 M CCl_4 are summarized in Table I. A notable feature is that the addition of CCl_4 to octane solutions has little influence on ϕ_f values measured under CO (1.0 atm). Furthermore, although ϕ_f measured under argon was found to be higher in CCl_4/octane than that in neat octane under argon, *the former value was several orders of magnitude smaller than that measured under CO in the same mixed solvent.*

For dinuclear complexes, one diagnostic test for the photofragmentation of metal–metal bonds (e.g., eq 2) has been the trapping of the metal radicals M· by chlorocarbons to give the respective chlorides M–Cl.[31,32] Photolysis (405 nm) of $Ru_3(CO)_{12}$ in a 1.0-M CCl_4 solution in octane under CO (1.0 atm) did indeed give a different product than found for photolysis in octane under CO. Prolonged photolysis led to bleaching of the 392-nm absorption band of $Ru_3(CO)_{12}$ and the deposition of a yellow solid. The resulting photolysis solution displayed IR bands at 2140 m, 2130 m, 2108 w, 2080 sh m, and 2074 s cm^{-1} while the solid when dissolved in CCl_4 displayed a closely analogous IR spectrum: 2141 s, 2132 m, 2109 w, 2085 sh s, and 2078 s cm^{-1}. With exception of the weak band at 2108 (9) cm^{-1}, these spectra are consistent with that of a mixture of two isomeric chloro complexes $Ru_2(CO)_6Cl_4$.[45] Dissolution of the yellow solid in THF gave a spectrum with bands at 2140 s, 2060 br s, and 1980 br s, cm^{-1} consistent with the spectrum of the adduct $Ru(CO)_3Cl_2(THF)$ which is formed from the reaction of $Ru_2(CO)_6Cl_4$ with THF.[45] Photolysis (405 nm) in neat CCl_4 solution gave the same products according to the IR spectra.

The chlororuthenium complexes, however, are *not* the primary photoproducts under CO. Infrared spectra taken periodically during the 405-nm photolysis of $Ru_3(CO)_{12}$ in a 1.0 M CCl_4 solution in octane demonstrated $Ru(CO)_5$ to be the initial product. Even after nearly complete photofragmentation of the starting material, the major metal carbonyl species present is $Ru(CO)_5$. Furthermore, when this solution was left in the dark, the bands attributed to the chlororuthenium species continued to increase at the expense of those attributed to $Ru(CO)_5$. Thus, the $Ru_2(CO)_6Cl_4$ products are, at least largely, the result of secondary thermal reactions of CCl_4 with $Ru(CO)_5$.

$$Ru(CO)_5 + CCl_4 \rightarrow Ru_z(CO)_xCl_y + ? \qquad (4)$$

The thermal reaction with CCl_4 was reaffirmed by preparing a solution of $Ru(CO)_5$ by the exhaustive photolysis of $Ru_3(CO)_{12}$ in octane under CO. The CCl_4 (CO saturated) was then added to give a 1.0-M solution, and the reaction was allowed to proceed in the dark at 23 °C. The reaction, monitored by disappearance of the ν_{CO} band of $Ru(CO)_5$ at 2000 cm^{-1}, gave a linear plot of $\ln(A_t - A_\infty)$ vs. time with a first-order rate constant (slope) of 1.2×10^{-4} s^{-1}. Qualitative studies showed similar solutions of $Ru(CO)_5$ in octane (P_{CO} = 1.0 atm) reacted rapidly with $CHBr_3$ and with CHI_3 to give *cis*-$Ru(CO)_4Br_2$ and *cis*-$Ru(CO)_4I_2$, respectively (identified from known IR spectra).[46] In contrast, the iron analogue $Fe(CO)_5$ proved much less reactive with CCl_4 (1.0 M) in octane solution, the upper limit for the rate being at least two orders of magnitude smaller than that for $Ru(CO)_5$. This observation parallels the previous report[47] that $Ru(CO)_5$ is three orders of magnitude more reactive than is $Fe(CO)_5$ toward oxidation by I_2 to give the respective diiodides $M(CO)_4I_2$.

Table III. Fragmentation and Substitution Quantum Yields for $Ru_3(CO)_{12}$ with Added $P(OCH_3)_3$

λ_{irr} (nm)	P_{CO} (atm)[a]	[$P(OCH_3)_3$] (M)	$10^3\phi_f$[b]	$10^3\phi_s$[b]
		In Octane Solution		
405	1.0	0.000	28 ± 4	*c*
	0.0	0.012	23 ± 1	*e*
366	0.0	0.012	25 ± 1	34 ± 1
334	0.0	0.012	21 ± 1	68 ± 8
313	0.0	0.012	24 ± 2	86 ± 3
	1.0	0.012	29 ± 2	43 ± 3
254	0.0	0.012	*c*	~120
		In Cyclohexane Solution		
405	0.0	0.0010	3.2 ± 0.6	*e*
	0.0	0.0050	11.0 ± 1.4	*e*
	0.0	0.010	18.3 ± 0.6	*e*
	0.0	0.10	42.0 ± 1.7	*e*
		In THF Solution		
405	1.0	0.000	3.5 ± 0.7	*c*
	0.0	0.012	3.0 ± 0.1	*e*
366	0.0	0.012	2.5 ± 0.1	16.5 ± 0.5
334	0.0	0.0030	*c*	50 ± 3
	0.0	0.012	4 ± 1	53 ± 2
	0.25	0.0030	2.0 ± 0.1	16 ± 5
	0.25	0.0060	3.3 ± 0.2	26 ± 2
	0.25	0.012	4 ± 1	32 ± 5
313	0.0	0.012	2.4 ± 0.3	78 ± 9
	0.25	0.012	2.8 ± 0.3	54 ± 5
	1.0	0.012	2.7 ± 0.3	39 ± 5
254	0.0	0.012	~3	~125

[a] T = 25 °C, total pressure was 1.0 atm with N_2 or argon making up the balance. [b] In mol per einstein. [c] Not determined. [d] P_{Ar} = 1.0 atm. [e] No substitution observed, a generous upper limit of one half ϕ_f can be estimated.

II. Photolysis of $Ru_3(CO)_{12}$ with Other Ligands. Ethylene. Photolysis (405 nm) of $Ru_3(CO)_{12}$ in octane solution equilibrated with ethylene (1.0 am) gives fragmentation to the mononuclear species $Ru(CO)_4(C_2H_4)$ (eq 5) as previously reported.[5] The quantum yield for this process was measured as 0.051 ± 0.004 mol/einstein.

$$Ru_3(CO)_{12} + 3C_2H_4 \xrightarrow{h\nu} 3Ru(CO)_4(C_2H_4) \qquad (5)$$

Trimethyl Phosphite. Photolysis (405 nm) of $Ru_3(CO)_{12}$ (1×10^{-4} M) in octane under Ar with a large excess of $P(OCH_3)_3$ (0.012 M) gave only the monosubstituted $Ru(CO)_4(P(OCH_3)_3)$ as initial product (eq 6). Only after more than 20% of the starting

$$Ru_3(CO)_{12} + 3P(OCH_3)_3 \xrightarrow{h\nu} 3Ru(CO)_4(P(OCH_3)_3) \qquad (6)$$

material had reacted were traces of the disubstituted mononuclear carbonyl detected in the IR spectra. The ϕ_f was measured as 0.023 ± 0.001 under these conditions but were shown to be markedly dependent on [$P(OCH_3)_3$] (Table III).

Although 405-nm photolysis of $Ru_3(CO)_{12}$ plus $P(OCH_3)_3$ in octane led to spectral changes consistent with photofragmentation as the only spectrally discernable reaction (Figure 1), photolysis at shorter wavelengths gave very different spectral changes (Figure

(45) Johnson, B. F. G.; Johnston, R. D.; Lewis, J. *J. Chem. Soc. A* **1969**, 792–797.

(46) Calderazzo, F.; L'Eplattenier, F. *Inorg. Chem.* **1967**, *6*, 1220–1224.
(47) Huq, R.; Poë, A. J.; Chawla, S. *Inorg. Chim. Acta* **1980**, *38*, 121–125.

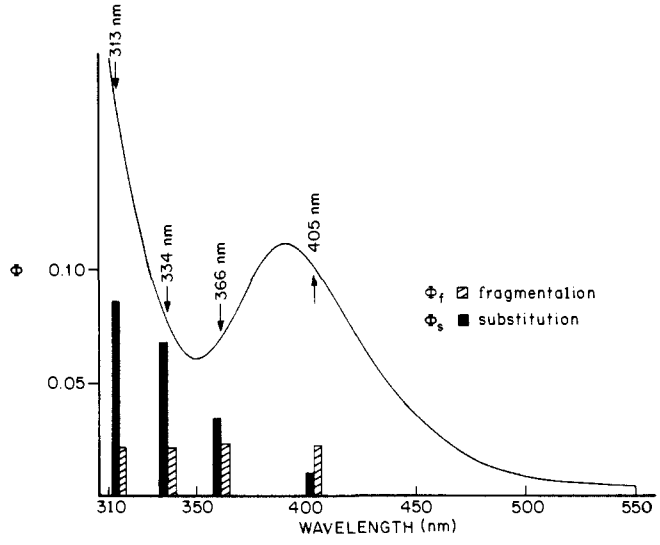

Figure 4. Spectrum of $Ru_3(CO)_{12}$ in octane solution and quantum yields for photosubstitution and photofragmentation in the presence of 0.012 M $P(OCH_3)_3$ as a function of irradiation wavelength.

2). According to the IR spectra, there were three initial products of the 313-nm photolysis of $Ru_3(CO)_{12}$ (1×10^{-4} M) plus $P(OCH_3)_3$ (2×10^{-2} M) in octane (1 atm Ar). These were $Ru(CO)_4(P(OCH_3)_3)$ (2050 and 2018 cm^{-1}),[39] $Ru_3(CO)_{11}(P(OCH_3)_3)$ (2072, 2002, 1971, and 1957 cm^{-1}),[40] and $Ru(CO)_3(P(OCH_3)_3)_2$ (1933 and 1923 cm^{-1}).[40] The quantum yields for the competing fragmentation and cluster-substitution pathways were determined for the early stages of the reaction, where it was assumed that the only cluster product was $Ru_3(CO)_{11}P(OCH_3)_3$ (λ_{max} 402 nm, ϵ_{max} 6.9×10^3). Thus, the fragmentation yield could be calculated from the optical density changes at 398 nm, the isosbestic point for the two cluster species. The photosubstitution yields ϕ_s for eq 7 were calculated from the absorbance changes at 380 nm once

$$Ru_3(CO)_{12} + P(OCH_3)_3 \xrightarrow{h\nu} Ru_3(CO)_{11}(P(OCH_3)_3) \quad (7)$$

the part attributable to photofragmentation was subtracted. The results of these calculations for other λ_{irr} are summarized in Table III and Figure 4. Notably, ϕ_f shows but small variations over the λ_{irr} range 405–313 nm while ϕ_s rises markedly over the same range. Photolysis under CO increased ϕ_f slightly but decreased ϕ_s substantially. It is also notable that continued photolysis progressively shifts the visible range absorption band to wavelengths beyond that of the monosubstituted product, consistent with further photoreaction to give polysubstituted products.

One possible route to substituted clusters would be from secondary photo- or thermal reactions of the photofragmentation products. Although this seemed unlikely given that the ϕ_s/ϕ_f ratio was constant over the early stages of the reaction, several control reactions were carried out to check this possibility. First, a solution of $Ru(CO)_4P(OCH_3)_3$ (10^{-3} M) plus $P(OCH_3)_3$ (10^{-2} M) in octane under Ar was photolyzed at 313 nm. The electronic spectra indicated that no cluster species were formed while the IR spectrum showed the photoproduct to be $Ru(CO)_3(P(OCH_3)_3)_2$ with a quantum yield of about 0.2. Continued photolysis gave IR spectral changes consistent with the formation of the trisubstituted mononuclear species. Second, no substituted clusters were observed when a mixture of $Ru_3(CO)_{12}$ (2×10^{-4} M) plus $Ru(CO)_4P(OCH_3)_3$ (10^{-3} M) were photolyzed at 313 nm under CO (1 atm).

Lastly, photolysis in THF, which quenches photofragmentation, gave a pattern of substitution yields with regard to λ_{irr}, to $[P(OCH_3)_3]$ and to CO similar to that in octane (Table III). Neither ϕ_f nor ϕ_s measured for 313-nm photolysis in THF were affected by the addition of the radical inhibitor 2,6-di(*tert*-butyl)-*p*-cresol. The consequence of THF suppressing ϕ_f but not ϕ_s is illustrated by comparing Figures 2 and 5. Prolonged 313-nm photolysis in THF leads to products with λ_{max} values to the red of the known trisubstituted species $Ru_3(CO)_9(P(OCH_3)_3$ (426 nm). When such

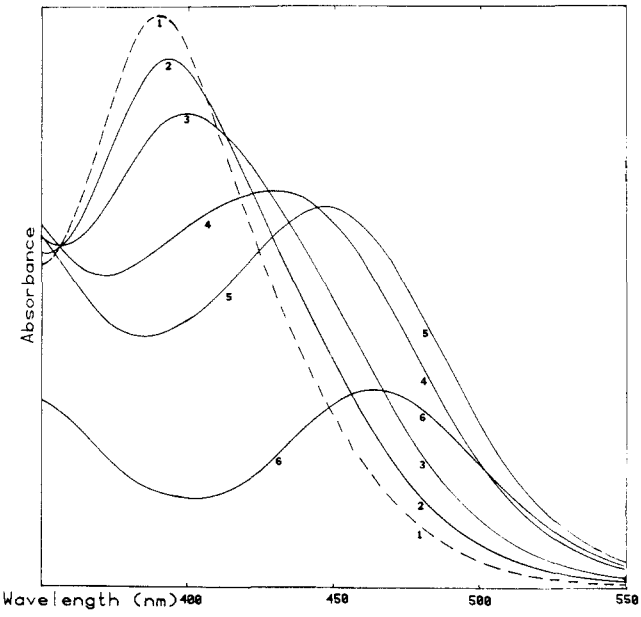

Figure 5. Sequential spectra recorder during the 313-nm photolysis of $Ru_3(CO)_{12}$ plus $P(OCH_3)_3$ (0.012 M) in THF solution. (1 is the initial spectrum.)

Table IV. Photofragmentation and Photosubstitution Quantum Yields for $Ru_3(CO)_{12}$ with Added PPh_3[a]

λ_{irr} (nm)	P_{CO} (atm)	$[PPh_3]$ (M)	$10^3\phi_f$[b]	$10^3\phi_s$[b]
		In Cyclohexane Solution		
405	1.0	0.000	19.0 ± 2	*c*
	1.0	0.0010	19.0 ± 2	*c*
	0.0	0.0010	2.8 ± 0.3	*c*
	0.0	0.010	16.0 ± 2	*c*
	0.0	0.10	36.0 ± 4	*c*
	1.0	0.10	40.0 ± 4	*c*
		In THF Solution		
405	0.0	0.012	2.0 ± 0.2	<5[d]
366	0.0	0.012	2.0 ± 0.7	18.5 ± 0.5

[a] T = 25 °C. [b] In mol per einstein. [c] Not determined owing to much larger contribution of alternate pathway. [d] Upper limit only, no substitution observed.

a solution was chromatographed by elution with THF from a silica gel column four reaction products were isolated, the first three being the mono-, di-, and trisubstituted clusters which were identified from their IR spectra and the respective λ_{max} (402, 416, or 426 nm) of the visible region absorption band and which eluted in the order of increasing substitution. The fourth species, the last to elute, displayed an absorption maximum at 450 nm, thus tetrasubstitution is suggested. The same product was observed when $Ru_3(CO)_9(P(OCH_3)_3)_3$ was photolyzed (260–380-bandpass filter) with an excess of $P(OCH_3)_3$ in THF under Ar.

Triphenyl Phosphines. The earlier studies of Johnson et al.[5] reported that photolysis (λ_{irr} > 390 nm) of $Ru_3(CO)_{12}$ in the presence of PPh_3 gave both singularly and doubly substituted mononuclear ruthenium carbonyls (eq 8). We have confirmed

$$Ru_3(CO)_{12} + PPh_3 \xrightarrow{h\nu} 2Ru(CO)_4PPh_3 + Ru(CO)_3(PPh_3)_2 \quad (8)$$

that photolysis under these conditions does indeed lead to the formation of both products; however, the product ratio as determined quantitatively by IR proved to be a function of the solution conditions. Photolysis (390-nm cutoff filter) of a 5×10^{-4} M $Ru_3(CO)_{12}$ solution in cyclohexane containing 5×10^{-3} M PPh_3 under Ar gave a 4/1 ratio of mono- to disubstituted products while photolysis with 4×10^{-2} M PPh_3 gave ratio close to two. However, under CO (1 atm) the only products found were $Ru(CO)_5$ and $Ru(CO)_4PPh_3$, the ratio being 1–3 in 8×10^{-3} M PPh_3. Quantum yields for photofragmentation (λ_{irr} 405 nm) in

Table V. Photofragmentation Quantum Yields for $Ru_3(CO)_{12-n}L_n$ in Cyclohexane Solution under CO (1.0 atm)

complex	λ_{max} (ϵ)[b]	$10^3 \times \phi_f$[c]
$Ru_3(CO)_{12}$	392 (7.7×10^3)	19 ± 1
$Ru_3(CO)_{11}(P(OCH_3)_3)$	402 (6.9×10^3)	44 ± 9
$Ru_3(CO)_{10}(P(OCH_3)_3)_2$	416 (7.6×10^3)	31 ± 2
$Ru_3(CO)_9(P(OCH_3)_3)_3$	426 ($7.6 \times t\ 10^3$)	5.2 ± 0.4
$Ru_3(CO)_{11}(P(p\text{-tolyl})_3)$	417 (7.64×10^3)	31 ± 4
$Ru_3(CO)_{10}(P(p\text{-tolyl})_3)_2$	390 (7.5×10^3), 493 (7.4×10^3)	21 ± 1
$Ru_3(CO)_9(P(p\text{-tolyl})_3)_3$	383 (1.0×10^4), 497 (9.8×10^3)	0.2 ± 0.1
$Ru_3(CO)_9(PPh_3)_3$	388 (1.1×10^4), 502 (1.2×10^4)	0.8 ± 0.4
$Ru_3(CO)_{11}(P(O(o\text{-tolyl}))_3)$	401 (5.2×10^3)	55 ± 3
$Ru_3(CO)_{10}(P(O(o\text{-tolyl}))_3)_2$	420 (7.0×10^3)	42 ± 2
$Ru_3(CO)_9(P(O(o\text{-tolyl}))_3)_3$	445 (9.1×10^3)	0.4 ± 0.09

[a] T = 25 °C. [b] λ_{max} in nm, ϵ in M^{-1} cm^{-1}. [c] In mol per einstein.

the presence of PPh_3 were also dependent on the concentration of this ligand (Table IV).

As noted above for CO and $P(OCH_3)_3$, the photofragmentation quantum yields (405 nm) with PPh_3 were an order of magnitude smaller in THF than in hydrocarbon solution. Photolysis at lower wavelengths in THF under Ar gave substantial photosubstitution to $Ru_3(CO)_{11}(PPh_3)$ (λ_{max} 404 nm), and prolonged photolysis resulted in a progressive substitution of the cluster to the bis- and tris-substituted triruthenium complexes. Photosubstitution quantum yields at different [PPh_3] are summarized in Table IV. Attempts to evaluate the possible photosubstitution reactions for λ_{irr} = 405 nm indicated that with high concentrations (>0.1 M) of PPh_3 photosubstitution occurred with a small limiting ϕ_s (about 0.01); however, the accuracy of this measurement was limited by the need to correct for the thermal substitutions which lead to comparable absorbance changes.

Given these results and the observation that the multiple substitution in the case of L = $P(OCH_3)_3$ is observed only after a significant fraction of the starting material has reacted, it was concluded that formation of disubstituted photoproducts $Ru(CO)_3L_2$ is the result of secondary photo- and thermal reactions. Several such processes are likely candidates. For example, the broad-band excitation used in the first experiments would have given significant photosubstitution of the cluster which on subsequent fragmentation would lead to disubstituted mononuclear complexes.

III. Photolyses of Substituted Clusters under CO. Table V summarizes the quantum yields for the photofragmentations of the clusters $Ru_3(CO)_{12-n}L_n$ (L = $P(OCH_3)_3$, PPh_3, or $P(p\text{-tolyl})_3$) under CO in cyclohexane. For each case, photosubstitution of CO for L was apparently negligible and photofragmentation followed the stoichiometry. The most notable feature of these

$$Ru_3(CO)_{12-n}L_n + 3CO \xrightarrow{h\nu\ (405\ nm)} (3-n)Ru(CO)_5 + nRu(CO)_4L \quad (9)$$

data is that mono- and bis-substituted complexes gave ϕ_f values comparable to that for $Ru_3(CO)_{12}$, but those for tris-substituted clusters were substantially smaller. A very small quantum yield for the photofragmentation of $Ru_3(CO)_9(PPh_3)_3$ has been previously noted qualitatively by Wrighton and co-workers.[18]

IV. Flash Photolysis of $Ru_3(CO)_{12}$. Experiments at Longer λ_{irr} (>395 nm). Flash photolysis of a $Ru_3(CO)_{12}$ solution in cyclohexane equilibrated with CO (P_{CO} 1.0 atm) showed some net photoreaction, but no transients were detectable with lifetimes in excess of the "deadtime" (about 20 μs) of the conventional xenon flash lamp apparatus used for these experiments. Neither observable transients nor net photochemistry resulted from a similar flash experiment of $Ru_3(CO)_{12}$ in neat cyclohexane equilibrated with argon. In contrast, a CO equilibrated cyclohexane solution of $Ru_3(CO)_{12}$ containing THF (1.0 M) displayed some transient bleaching in the spectral region 380–460 nm which decayed exponentially (k_d = 20 ± 5 s^{-1}) to give a final absorbance consistent with a small amount of net photoreaction. The same transient

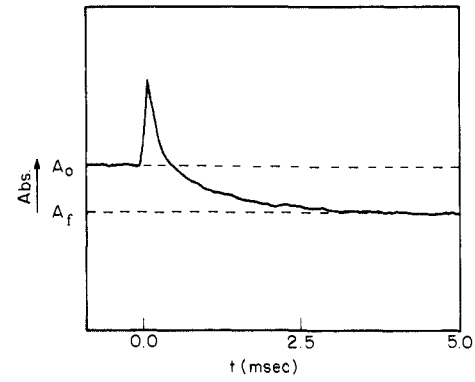

Figure 6. Absorbance (λ_{mon} = 480 nm) vs. time trace for the longer wavelength flash photolysis (λ_{irr} > 395 nm) of a cyclohexane solution of $Ru_3(CO)_{12}$ plus $P(OCH_3)_3$ (0.010 M).

behavior with an identical k_d value was noted for an analogous THF/cyclohexane solution under argon with the exceptions that considerably more bleaching was apparent immediately after the flash and that no net photochemistry was seen. Lastly, the identical transient kinetics were noted in neat THF solution. These results can be interpreted in terms of the formation of an intermediate (or excited state) which can be trapped by CO to give fragmentation products or by THF to give a longer lived intermediate which decays largely back to $Ru_3(CO)_{12}$.

$$Ru_3(CO)_{12} \xrightarrow{h\nu} I \begin{cases} \xrightarrow{+CO} \text{fragmentation products} \\ \xrightarrow{+THF} I' \end{cases} \quad (10)$$

$$I' \longrightarrow Ru_3(CO)_{12} \quad (11)$$

Similar transient bleaching at 390 nm followed by exponential decay to a final absorbance was seen in argon equilibrated cyclohexane solutions containing cyclohexene, PPh_3, or $P(OCH_3)_3$ flash photolysis with added cyclohexene leading to just small net photoreaction but photolysis added PPh_3 or $P(OCH_3)_3$ leading to net cluster fragmentation. No transients sufficiently long lived to be observed via this technique were found in neat cyclohexane under ethylene (1 atm), although net photofragmentation was significant. Notably, THF and cyclohexene were shown to be inhibitors of photofragmentation under continuous photolysis conditions (above) while the other three ligands and CO all participated readily in this photoreaction.

In the cases of cyclohexene, $P(OCH_3)_3$, and PPh_3, the flash photolysis kinetics were more conveniently investigated in the wavelength range 450–500 nm where the transients displayed greater absorbances than $Ru_3(CO)_{12}$. Given the net photochemistry seen in the presence of the latter two ligands, spectral changes at 390 nm involve first a flash induced absorbance decrease followed by further absorbance decay to products. In contrast, at 480 nm there is first a flash induced absorbance increase followed by exponential decreases to the product spectrum (Figure 6). For $P(OCH_3)_3$, increases of this ligand's concentration (0.005–0.05 M) did not effect k_d but did increase the amount of transient formed and the extent of net photoreaction. The k_d values determined for the various donor ligands follow the order THF < cyclohexene < PPh_3 < $P(OCH_3)_3$ and are summarized in Table VI.

Experiments at Shorter λ_{irr} (>315 nm). Flash photolysis of $Ru_3(CO)_{12}$ at the shorter wavelengths was carried out both in THF solution and in cyclohexane solutions. In the absence of added CO or other ligands, flash excitation of $Ru_3(CO)_{12}$ in THF led to the formation of an insoluble material believed to be the ruthenium carbonyl polymer noted above. In contrast, flash photolysis in THF under excess CO was well-behaved with a very small amount of net fragmentation noted as the only *net* photoreaction in agreement with continuous photolysis behavior under analogous conditions. However, the shorter wavelength flash excitation did lead to the observation of a transient with absorbance in the wavelength range 480–550 nm which decayed exponentially

Table VI. First-Order Rate Constants for Decay of Transients Seen by Longer Wavelength (λ_{irr} > 390 nm) Flash Photolysis of $Ru_3(CO)_{12}$ in Cyclohexane Solutions with Various Added Ligands[a]

ligand	concentration (M)	k_d (s^{-1})	comments
none		>5 × 10^4 [b]	no net photoreaction
CO	0.0084[c]	>5 × 10^4 [b]	net photofragmentation
$H_2C{=}CH_2$	*d*	>5 × 10^4 [b]	net photofragmentation
$P(OCH_3)_3$	0.005–0.05	900 ± 30	net photofragmentation
PPh_3	0.005–0.01	200 ± 30	net photofragmentation
cyclohexene	0.01	59 ± 10	no net photoreaction
THF/CO	[THF] = 1.0[b]	20 ± 5	small net photofragmentation
THF	1.0	20 ± 5	no net photoreaction

[a] T = 25 °C. [b] No transient seen, estimated rate is lower limit for first order reaction obscured by flash. [c] P_{CO} = 1.0 atm (see Table I). [d] $P_{C_2H_4}$ = 1.0 atm. [e] Identical behavior noted in neat THF solution.

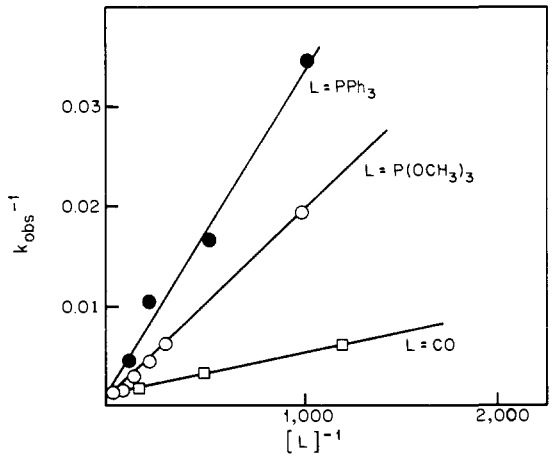

Figure 7. Double reciprocal plots of the kinetics data obtained for the decay of the transients seen for the short wavelength flash photolysis (λ_{irr} > 315 nm) of THF solutions of $Ru_3(CO)_{12}$ in the presence of various ligands L.

back to the starting spectrum with a [CO] dependent k_{obsd}. The spectral properties of this transient are considerably different than the transient noted under similar conditions when longer λ_{irr} flash excitation (>395 nm) was used, since the latter gave no observable absorbance increases in this region. However, when the shorter λ_{irr} flash photolysis experiment was monitored at 390 nm, temporal absorbance changes were consistent with those expected for the simultaneous formation of two transients.

The kinetics properties of the new transient from the shorter wavelength flash excitation were, therefore, monitored at 480 nm. The plot of k_{obsd} vs. [CO] was curved, but the double reciprocal plot (k_{obsd}^{-1} vs. $[CO]^{-1}$) was linear with a nonzero intercept (Figure 7).

Short λ_{irr} flash photolysis of $Ru_3(CO)_{12}$ in argon flushed THF solution with excess added PPh_3 or $P(OCH_3)_3$ and also gave initial transient absorptions at these monitoring wavelengths similar to those noted under CO. However, in these cases, the system was shown to undergo further absorbance increases to a final product spectrum consistent with net reaction to give, principally, the substituted clusters $Ru_3(CO)_{11}L$. Plots of ln ($A_\infty - A_t$) vs. time for these processes were linear with [L] dependent k_{obsd} values. The double reciprocal plots (k_{obsd}^{-1} vs. $[L]^{-1}$) were linear in each case (Figure 7), and the values of the slopes and intercepts of these are summarized in the Discussion.

The shorter wavelength flash photolysis experiments carried out in cyclohexane solutions gave a very different pattern. Under CO (1.0 atm) *no* transients with lifetimes longer than that of the flash (20 μs) were seen, only net absorbance decreases at 390 nm and longer wavelengths indicating some fragmentation. In the presence of $P(OCH_3)_3$ or PPh_3, immediate shifts in the absorption were observed indicating the formation of substitution products within the flash lifetime. In addition, there were temporal absorbance decreases at 390 nm and at 480 nm with the exponential decay kinetics behavior identical with that seen above for the photofragmentation precursor after longer wavelength flash excitation under analogous conditions. Thus, it appears that in cyclohexane any transient precursors to photosubstitution products are much shorter lived than in THF.

Discussion

The above results clearly demonstrate that two independent photoreactions are the consequence of the photoexcitation of $Ru_3(CO)_{12}$ in solution. Longer wavelength (>400 nm) excitation in the presence of added CO or other ligands leads almost exclusively to photofragmentation into mononuclear complexes (e.g., eq 1), while higher energy excitation also leads to photosubstitutions of the intact cluster. The photofragmentation pathway is consistent with the interpretation of the lowest energy absorption band at 392 nm (the "$\sigma \rightarrow \sigma^*$ band") in terms of a transition from an orbital having strong metal–metal bonding contributions to one which is largely antibonding with respect to the metal–metal bonding framework of the cluster.[34,35] Furthermore, the photosubstitution behavior is consistent with the proposal that the shoulder on the rising absorption below 350 nm represents a transition to an orbital displaying considerable antibonding character with respect to metal–ligand interactions.[34,35]

Notably, in both hydrocarbon and THF solution the quantum yields for fragmentation in the presence of a constant concentration of $P(OCH_3)_3$ (0.012 M) proved to be essentially independent of λ_{irr}. A similar observation has been reported by Poë[28] who found that ϕ_f under a constant P_{CO} was independent of λ_{irr} in isooctane solution. These results can be viewed in terms of fragmentation occurring from a lowest energy excited state or a common lower energy state formed efficiently via internal conversion from higher energy states populated by direct excitation. The relatively low quantum yield for fragmentation (only 2–5% in hydrocarbon solutions, an order of magnitude smaller in THF solution, see below) suggests that this state and/or subsequent intermediates formed along the reaction coordinate largely decay back to $Ru_3(CO)_{12}$ and undergo fragmentation only inefficiently. Some modest decreases in ϕ_f are apparent at lower λ_{irr} reflective of the competing path to substitution products at these wavelengths, but the experimental uncertainties are comparable to the expected deviations.

The marked wavelength dependence of the photosubstitution quantum yields (Tables III and IV) would be consistent with the direct reaction from a upper level excited state prior to internal conversion to the state(s) responsible for fragmentation. Such λ_{irr} dependence may reflect the extent the transition leading to the substitution active state overlaps with other absorption bands (e.g., the lowest energy $\sigma \rightarrow \sigma^*$ band) having different reactivity properties. It is also possible that the CO labilization occurs from vibrationally nonequilibrated electronic states leading to higher ϕ_s at shorter λ_{irr}. However, the failure to see significant substitution at 405 nm indicates that an electronic state other than that leading to fragmentation is responsible for the ligand dissociation (see below).

The Photofragmentation Pathway. Given that metal–metal bonded dimers often undergo efficient homolytic bond cleavage upon photoexcitation,[30,31] a logical proposal for the first step for photofragmentation mechanism of trinuclear clusters would be the formation of a diradical via the homolysis of one metal–metal bond. However, the results of photolysis in CCl_4 solution and

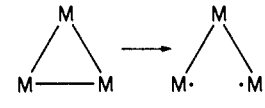

in octane solution to which CCl_4 had been added clearly indicate that a diradical sufficiently long-lived to be trappable in the manner seen in metal–dimer systems is not formed with $Ru_3(CO)_{12}$. Under an argon atmosphere, photofragmentation yields in the presence of CCl_4 are only marginally larger than in the absence of CCl_4 (Table I) and are orders of magnitude smaller than for analogous CCl_4 solutions under CO, despite the fact that CO is not required in the stoichiometry for the formation of chloro-

carbonyl ruthenium products. Furthermore, the fact that photolysis in CCl_4 containing solutions under CO results first in $Ru(CO)_5$ formation followed by the thermal reaction of this mononuclear species to give chloro derivatives clearly demonstrates that the latter products are the result of a secondary thermal reaction and do not reflect the reactivities of photochemically generated metal radicals.

The dominant feature of the longer λ_{irr} CW photolysis experiments is the role of two-electron donors. Ligands (L) which are π-acids such as CO, ethylene, or activated olefins (e.g., dimethyl maleate) and phosphorous donors PR_3 (triphenyl phosphine or trimethyl phosphite) each give modest quantum yields for eq 12 in hydrocarbon solutions. These ϕ_f values are [L] dependent.

$$Ru_3(CO)_{12} + 3L \xrightarrow{h\nu} 3Ru(CO)_4L \qquad (12)$$

In contrast, virtually no photoactivity was noted when L is a harder donor such as THF, diglyme, or 2-methyltetrahydrofuran present either as the solvent or as an additive to hydrocarbon solutions. Although the low photoreactivity might be attributed to instability of the mononuclear species in these latter cases, such an interpretation would not explain the observation that these ligands also serve as Stern–Volmer type quenchers of the photofragmentation chemistry in the presence of CO or PR_3.

Such characteristics led to the proposal (in two independent preliminary reports,[28,2a]) that the mechanism for the fragmentation pathway must involve the formation of an intermediate with the same composition of the starting cluster (i.e., an isomeric form of $Ru_3(CO)_{12}$) capable of first order return to the initial cluster or of capture by a two electron donor. The diradical A would satisfy the first criterion but both the failure of the photoreaction intermediates to undergo trapping by CCl_4 as well as the required reactivity with Lewis type bases argue against the diradical formulation.[48] An alternative structure satisfying these criteria is I which would be formed by the heterolytic cleavage of a Ru–Ru bond and corresponding movement of a carbonyl from a terminal site to a bridging one to maintain the electrical charge neutrality of both Ru atoms. The result would be to leave one of the ruthenium atoms electron deficient (a 16 electron species) and capable of coordinating a two electron donor. (Alternatively, I may have a hydrocarbon solvent molecule coordinated at the electron deficient ruthenium.[49])

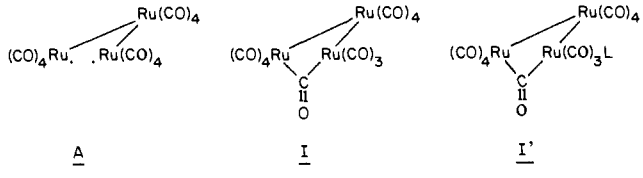

A I I'

Other authors,[9,12] in interpreting CW photolysis experiments with both $Ru_3(CO)_{12}$ and $Os_3(CO)_{12}$ in the presence of activated olefins such as methylacylate, have proposed that the fragmentation of such trinuclear clusters occurs via the sequential cleavage of two metal–metal bonds (perhaps via A) to form mononuclear and dinuclear fragments. These authors presented evidence[12] for the formation of a trappable dinuclear species $M_2(CO)_8$ and have suggested[9] the possible formation of $Ru(CO)_4$, e.g., eq 13.

$$Ru_3(CO)_{12} \xrightarrow{h\nu} \rightarrow Ru(CO)_4 + Ru_2(CO)_8 \qquad (13)$$

However, if $Ru(CO)_4$ were formed via eq 13, the process could not be reversible given the independence of ϕ_f to the irradiation intensity as observed by Poë and co-workers.[28] Furthermore, this mechanism would be inconsistent with the flash photolysis kinetics described below.

Scheme I illustrates a proposed mechanism for the photofragmentation pathway via an intermediate such as I. If it is

Scheme I

$$Ru_3(CO)_{12} \underset{k_d}{\overset{h\nu}{\rightleftharpoons}} [Ru_3(CO)_{12}^*] \xrightarrow{k_f} I \qquad (14)$$

$$I \xrightarrow{k_1} Ru_3(CO)_{12} \qquad (15)$$

$$I + L \underset{k_3}{\overset{k_2}{\rightleftharpoons}} \underset{I'}{Ru_3(CO)_{12}L} \qquad (16)$$

$$I' \xrightarrow{k_4} Ru(CO)_4L + Ru_2(CO)_8 \xrightarrow{+\,2L,\ fast} 3Ru(CO)_4L \qquad (17)$$

$$I' \xrightarrow{k_5} Ru_3(CO)_{12} + L \qquad (18)$$

assumed that k_3 is much smaller than $k_4 + k_5$ (see below), then the value of ϕ_f is determined by three pairs of competitive processes. The first is the formation of I from the excited state in competition with decay to $Ru_3(CO)_{12}$ and occurs with an efficiency determined by the ratio $k_f/(k_f + k_d)$ (defined for the subsequent discussion as ϕ_I). The second represents the competition between decay of I back to $Ru_3(CO)_{12}$ (eq 15) and capture of I by L to give I′ (eq 16). The third represents the competitive reactions of I′ via eq 18 to reform $Ru_3(CO)_{12}$ and fragmentation via eq 17 to give $Ru(CO)_4L$ plus $Ru_2(CO)_8$ (which reacts rapidly to form the final mononuclear products). According to this model, ϕ_f is defined by

$$\phi_f = \phi_I\left(\frac{k_2[L]}{k_1 + k_2[L]}\right)\left(\frac{k_4}{k_4 + k_5}\right) \qquad (19)$$

This predicts that a plot of ϕ_f^{-1} vs. $[L]^{-1}$ will be linear with an intercept $(k_4 + k_5)/(\phi_I k_4)$ and a slope $(k_1/k_2)(k_4 + k_5)/(\phi_I k_4)$. For photofragmentation in cyclohexane with L = PPh_3 or $P(OCH_3)_3$ (0.001 to 0.1 M), this treatment gave linear plots with intercepts of 25 ± 2 and 23 ± 3 plus slopes of 0.35 and 0.29 M, respectively. The reciprocals of the intercepts represent the limiting ϕ_f values (0.040 ± 0.004 and 0.044 ± 0.006, respectively) at high [L], i.e., $\phi_I k_4/(k_4 + k_5)$. Notably, Poë, using a similar treatment concluded that ϕ_f(lim) in cyclohexane under various CO pressures has the value 0.051 ± 0.008 for 366-nm CW photolysis.[28] (We also noted some curvature in ϕ_f vs. [CO] plots for 405-nm excitation in cyclohexane but found the effects too small and the uncertainties too large over the P_{CO} range available to find the double reciprocal plots in this case convincing). According to the above analysis the intercept to slope ratio in each case is equal to k_2/k_1 and the values of 112, 79, and 71 M^{-1} are the results for CO, $P(OCH_3)_3$, and PPh_3, respectively. Given that k_1 would be independent of the identity of L, these values can be used to calculate the relative values for k_2 as 1.6 ± 0.3, 1.1 ± 0.2, and 1.0 ± 0.1 for CO,[50] $P(OCH_3)_3$, and PPh_3. These data are consistent with the nature of I proposed, i.e., a coordinatively unsaturated or weakly solvated species which is essentially unselective in reacting with available ligands.

Flash photolysis of $Ru_3(CO)_{12}$ in neat cyclohexane under argon, under CO (1 atm) or under C_2H_4 (1 atm) gave no detectable transients and in the latter two cases indicated the immediate formation of products within the flash lifetime. Thus, we can conclude that I, $Ru_3(CO)_{13}$ and $Ru_3(CO)_{12}(C_2H_4)$, if formed

(48) (a) A referee has suggested that the kinetics and quantum yield behavior noted here would be consistent with the diradical mechanism where A would react with two electron donors L to give a $17e^-/19e^-$ intermediate $\cdot Ru(CO)_4Ru(CO)_4Ru(CO)_4L\cdot$. The stimuli of this suggestion were the recent demonstrations (ref 48b) that mononuclear $17e^-$ organometallic radicals undergo associative substitution reactions, and it was further suggested that A may well be too short-lived to be reactive with CCl_4. Indeed the flash photolysis kinetics and the quantum yield behavior would be consistent with I being A and I′ being the $17e^-/19e^-$ diradical. However, the latter diradical should also be reactive with CCl_4, yet photofragmentation quantum yields for $Ru_3(CO)_{12}$ in octane solutions containing 1 M THF (where I′ has a lifetime of about 50 ms, Table VI) are little affected by the presence of CCl_4 (Table I). Thus, it appears unlikely that I′, which apparently is formed by the reaction of I with a two-electron donor such as THF, is a radical species. The simplest (but not necessarily exclusive) interpretation would be that I itself is also not a radical. (b) Basolo, F. *Inorg. Chem. Acta* **1985**, *100*, 33–40, and references therein.

(49) (a) Bonneau, R.; Kelly, J. M. *J. Am. Chem. Soc.* **1980**, *102*, 1220–1221. (b) Kelly, J. M.; Hermann, H.; Koerner von Gustorf, E. *J. Chem. Soc., Chem. Commun.* **1973**, 105–106.

(50) Calculated from data reported in ref 28.

under these conditions, decay with lifetimes less than the dead time of the flash apparatus (20 μs). The fact that no net photofragmentation was measurable under argon indicates that eq 15 is the sole pathway for the decay of I in the absence of added ligands and that k_1 has a lower limit of about 5×10^4 s^{-1} according to the above model. From the k_2/k_1 ratios of about 10^2 M^{-1} noted above, a lower limit for k_2 of about 5×10^6 M^{-1} s^{-1} can be estimated. This value can be compared to the second-order rate constant of $(3 \pm 1) \times 10^6$ M^{-1} s^{-1} reported for the reaction of flash photolysis generated $Cr(CO)_5$ with CO in cyclohexane solution.[49]

For L = PPh_3 or $P(OCH_3)_3$, flash photolysis of $Ru_3(CO)_{12}$ in cyclohexane gave absorbance changes indicating the immediate formation of a transient species which reacted further to give net photofragmentation. In the context of the above scheme, these transients should be $Ru_3(CO)_{12}L$ (I'). If it is assumed that eq 16 is a rapidly established equilibrium with the constant $K' = k_2/k_3$, the decay of I would follow the rate law

$$\frac{d[I']}{dt} = -\left(k_4 + k_5 + \frac{k_1}{K'[L]}\right)[I'] \qquad (20)$$

$$k_{obsd} = k_4 + k_5 + \frac{k_1}{K'[L]} \qquad (21)$$

For both $P(OCH_3)_3$ and PPh_3, k_{obsd} proved independent of [L] (Table VI), thus one may conclude that, under these conditions, the third term in k_{obsd} is insignificant and that $k_{obsd} = k_4 + k_5$. The decay of I' must occur in this case via eq 17 and 18 but with rates several orders of magnitude less than the lower limits of decay for comparable species when L = C_2H_4 or CO. On the basis of the experimentally indistinguishable ϕ_f(lim) values for L = CO, $P(OCH_3)_3$, or PPh_3, one can conclude that k_4 is substantially larger than k_5 for these ligands, although the modest differences in these values might be argued to imply a modest k_5 contribution to k_{obsd} for the latter two ligands. An alternative possibility would be that the k_4/k_5 ratio is essentially identical for all three ligands, a possibility which seems rather unlikely owing to the very different natures of the two processes.

A different situation obtains for photolysis with ligands such as THF and cyclohexene which lead to little net photoreaction under flash or CW excitation. For these ligands, the relatively long-lived transients must largely decay via pathways other than eq 17, therefore, $k_4 \ll k_5 + k_1/K'[L]$. The absence of any [L] dependence on the decay rate suggests that for these cases eq 18 is the principal pathway for decay and that $k_{obsd} \simeq k_5$.

The behavior of THF and other donor ligands as Stern–Volmer type quenchers of photofragmentation under CO can be analyzed according to the model in Scheme I by assigning L = CO and adding the following equations to represent the behavior of another ligand X where eq 22 and 23 are analogues to eq 16 and 18,

$$I + X \underset{k_3'}{\overset{k_2'}{\rightleftharpoons}} \underset{I''}{Ru_3(CO)_{12}X} \qquad (22)$$

$$I'' \xrightarrow{k_5'} Ru_3(CO)_{12} + X \qquad (23)$$

respectively, for X = THF, etc. If it is assumed that $(k_2'/k_3')[X]$ is large and that the primary decay mode for I'' is eq 23 and for I is eq 17, then the quantum yields for fragmentation are determined by the competition between CO and X for I, e.g.,

$$\phi_f = \phi_I \frac{k_2[CO]}{k_1 + k_2[CO] + k_2'[X]} \qquad (24)$$

Therefore the ratio ϕ_f^0/ϕ_f (where ϕ_f^0 is the quantum yield for fragmentation under CO in the absence of X) will have the form

$$\frac{\phi_f^0}{\phi_f} = I + \frac{k_2'}{k_1 + k_2[CO]}[X] \qquad (25)$$

Thus Stern–Volmer type plots (ϕ°/ϕ vs. [X]) should be linear as seen in Figure 3 with unit intercepts and slopes (K_{sv}) equal to $k_2'/(k_1 + k_2[CO])$. This predicted [CO] dependence of the K_{sv}'s was confirmed by the plots in Figure 3 for THF quenching under different P_{co} in cyclohexane. Analysis by plotting K_{sv}^{-1} vs. [CO] gave the ratios $k_2'/k_1 = 87$ M (intercept^{-1}) and $k_2/k_2' = 1.45$ (slope). The latter value reaffirms the conclusion above that I is rather unselective in its reactions with various donors in solution. Lastly, the slope/intercept ratio equals k_2/k_1 according to this model, and the value so calculated is 126 M^{-1}, essentially identical with that (112 M^{-1}) calculated above from Poë's ϕ_f [CO] dependence data.

Of some concern is the prediction according to eq 24 that ϕ_f should fall to zero at high [X] if the only decay pathway open to I'' were eq 23. Given that residual photoactivity in the presence of CO was noted even in THF solution, there must be an alternative, minor pathway for fragmentation. One such alternative would be for I'' to undergo a small amount of fragmentation via a pathway analogous to eq 17 and for the resulting, relatively unstable, $Ru(CO)_4X$ products to undergo further reaction with CO to give stable mononuclear products. Given the very small quantum yields for the residual ϕ_f in THF, it is not surprising that evidence for such a pathway was not found in the flash photolysis experiments.

For L = cyclohexene (1.0 M in octane solution) a small amount of photofragmentation was found even in the absence of CO (Table I). Thus about 6% of the decay of I'' must occur via fragmentation, and given a k_{obsd} value of 59 s^{-1}, the k_4 rate constant can be estimated at about 4 s^{-1}. In this context, the apparent values of k_4 fall into the sequence: CO, $CH_2{=}CH_2 \gg P(OCH_3)_3 > PPh_3 \gg$ cyclohexene > THF. This order qualitatively parallels π-acidity/σ donor properties of L, the faster rates being found for the stronger π-acids.[51] One possible interpretation of this observation would be that the activation barrier for the reaction of I' to form the initial fragmentation products ($Ru(CO)_4L$ plus $Ru_2(CO)_8$?) is higher for a stronger σ-donor (weaker π-acceptor) ligand owing to the electron-withdrawing character of the bridging CO of this intermediate.

The photofragmentation reactions of the substituted clusters $Ru_3(CO)_{12-x}L_x$ are characterized by quantitative reactivities similar to that of $Ru_3(CO)_{12}$ for $x = 1$ or 2 regardless of whether L = $P(OCH_3)_3$, $P(p\text{-tolyl})_3$, or $P(O(o\text{-tolyl}))_3$. However, for $x = 3$, in each case ϕ_f was orders of magnitude smaller (Table V)8, the relative differences between the cases $x = 2$ and $x = 3$ being much larger for the bulkier ligands $P(p\text{-tolyl})_3$ and $P(O(o\text{-tolyl}))_3$. These observations would be consistent with the model described in Scheme I, since the intermediate corresponding to I for the $Ru_3(CO)_9L_3$ species would be expected to be less reactive with solution phase CO (to give the I' equivalent) owing to the presence of the bulky L on each metal center. An alternative explanation[34] is that ligand substitution has led to a reversal in the excited state order so that the type of excited state responsible for the modest photofragmentation in $Ru_3(CO)_{12}$ is no longer the lowest excited state in trisubstituted derivatives. We view this explanation as somewhat unlikely given the smooth progression in the λ_{max} of the dominant lowest energy absorption band from $x = 0$ to 1 to 2 to 3 but the sharp discontinuity in ϕ_f between $x = 2$ and $x = 3$ (Table V).

The Photosubstitution Pathway. The photosubstitution pathway was primarily investigated in THF solution since fragmentation is largely suppressed in this medium while substitution yields were little affected (Table III). Besides the wavelength dependence discussed above, the other key observations are the transient seen by short wavelength flash photolysis and the effects of ligand identity and concentration on the lifetime of this intermediate and on ϕ_s. These data are interpretable in terms of a reaction scheme where the primary photoreaction is the dissociation of CO to give first a $Ru_3(CO)_{11}$ intermediate (II) then the solvated species

(51) (a) For example, Tolman and co-workers (ref 50b, c, and d) have demonstrated that the affinity of L for a zero-valent nickel center follows the order $CH_2{=}CH_2 > P(OCH_3)_3 > PPh_3 >$ cyclohexene and attributed the bulk of the differences qualitatively to the decreasing π-acidity over this series. (b) Tolman, C. A. *J. Am. Chem. Soc.* **1974**, *96*, 2780–2789. (c) Tolman, C. A.; Reutter, D. W.; Seidel, W. C. *J. Organomet. Chem.* **1976**, *117*, C30–33. (d) Tolman, C. A.; Seidel, W. C.; Gosser, L. W. *Organometallics* **1983**, *2*, 1391–1396.

$Ru_3(CO)_{11}S$ (II'). The relative solvent independence of ϕ_s

Scheme II

$$Ru_3(CO)_{12} \xrightarrow{h\nu} \underset{II}{Ru_3(CO)_{11}} + CO \quad (26)$$

$$II + S \underset{k_{-s}}{\overset{k_s}{\rightleftharpoons}} \underset{II'}{Ru_3(CO)_{11}S} \quad (27)$$

$$II + CO \xrightarrow{k_{co}} Ru_3(CO)_{12} \quad (28)$$

$$II + L \xrightarrow{k_L} Ru_3(CO)_{11}L \quad (29)$$

supports the view that the first step is CO dissociation rather than an associative displacement by solvent or another ligand. The decrease in ϕ_s when the shorter wavelength photolyses were carried out under CO would, therefore, be explained in terms of the trapping of II by CO (eq 28) in competition with trapping by L (eq 29). In this context, ϕ_s should respond to variation in [L] and [CO] according to

$$\phi_s = \phi_{II}\frac{k_L[L]}{k_{co}[CO] + k_L[L]} \quad (30)$$

A plot of ϕ_s^{-1} vs. $[L]^{-1}$ should, therefore, give ϕ_{II}^{-1} as an intercept and $k_{co}[CO]/k_L$ as the slope. Such treatment of the data for 334-nm photolysis of $P(OCH_3)_3$ solutions gave a limiting ϕ_s of 0.057 ± 0.017 and a k_{co}/k_L ratio of 4.1 ± 1.4 under these conditions. The ϕ_s(lim) agrees within experimental uncertainty with the $[P(OCH_3)_3]$ independent ϕ_s values measured under argon, i.e., about 0.053.

The transient seen by flash photolysis in THF is undoubtedly II' (S = THF), since no transient precursor to substitution with a lifetime >20 μs was seen in cyclohexane despite the comparable ϕ_s in both solvents. According to Scheme II, the rate law for the disappearance of the THF adduct II' would be

$$\frac{d[II']}{dt} = \frac{-(k_{co}[CO] + k_L[L])k_{-s}[II]}{k_s + k_{co}[CO] + k_L[L]} \quad (31)$$

For L = CO or [L] ≫ [CO], this simplifies to

$$\frac{d[II']}{dt} = \frac{-k_L k_{-s}[L][II']}{k_s + k_L[L]} \quad (32)$$

giving a relationship between [L] and the flash photolysis measured k_{obsd}

$$k_{obsd} = \frac{k_L k_{-s}[L]}{k_s + k_1[L]} \quad (33)$$

A plot of k_{obsd}^{-1} vs. $[L]^{-1}$ is predicted to be linear with slope $= k_s/k_{-s}k_L$ and a nonzero intercept k_{-s}^{-1} as seen in Figure 7. Slopes of $(4.0 \pm 0.1) \times 10^{-6}$, $(2.1 \pm 0.2) \times 10^{-5}$, and $(3.2 \pm 0.3) \times 10^{-5}$ mol s/L were measured for L = CO, $P(OCH_3)_3$, and PPh_3, respectively while intercepts of $(1.0 \pm 0.6) \times 10^{-3}$, $(0.5 \pm 0.3) \times 10^{-3}$, and $(1.1 \pm 0.2) \times 10^{-3}$ s, respectively, were the results for the same ligands. From the intercepts, a k_{-s} value of about 10^3 s^{-1} can be estimated for the dissociation of THF from $Ru_3(CO)_{11}$(THF). The relative values of k_L can be determined from ratios of the slopes given that k_s/k_{-s} should be ligand independent. These relative values, normalized to that for PPh_3, are 8 ± 1, 1.5 ± 0.3, and 1.0 for CO, $P(OCH_3)_3$, and PPh_3, respectively. The ratio k_{co}/k_L for L = $P(OCH_3)_3$ is 5.3 ± 1, within experimental uncertainty of that derived from the 334-nm CW experiments described above. Thus the model for the photosubstitution reactions is self-consistent with both the CW and flash data.

It is interesting to note that the photosubstitution intermediate II appears to be significantly more selective toward reaction with various two electron donor substrates than is the photofragmentation intermediate I. One speculative rationalization of this is

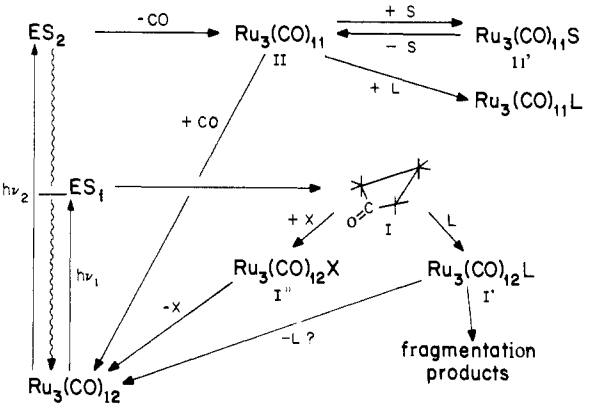

Figure 8. Qualitative model for the photoreactions of $Ru_3(CO)_{12}$.

that the $Ru_3(CO)_{11}$ intermediate has the opportunity to "delocalize" its unsaturation by having one CO bridge an edge of the metal triangle with concommitant formation of a multiple metal–metal bond, i.e.,

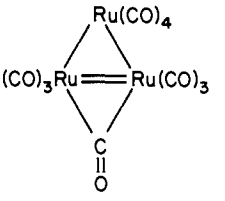

A similar rearrangement is not accessible to I.

Summary

Figure 8 summarizes many of the conclusions drawn here. Electronic excitation of $Ru_3(CO)_{12}$ solutions under CO or in the presence of PPh_3 or $P(OCH_3)_3$ leads to two photoreactions, fragmentation to mononuclear products, and ligand substitutions. Quantum yields for the latter process are markedly wavelength dependent, very small or indetectable at longer wavelengths (>400 nm) but becoming the dominant pathway for UV excitation. This is proposed to be the result of reaction from an upper excited state ES_2. The photofragmentation pathway is dominant for longer wavelength excitation and is proposed to occur from the lowest energy excited state ES_1. Photofragmentation is quenched according to Stern–Volmer type kinetics by donor ligands such as THF, diglyme, and cyclohexene but ϕ_f values are little affected by the presence of CCl_4. Given that $Ru(CO)_5$ is the initial photoproduct even in 1 M CCl_4, it was concluded that metal–metal bond cleavage does not occur homolytically to give trappable metal radicals. Instead a mechanism is proposed in which fragmentation occurs via a nonradical intermediate (I) isomeric to the starting cluster and formed with a limiting quantum yield of about 0.05 mol/einstein at 405 nm. This is proposed to have one coordinatively unsaturated ruthenium center which reacts rather nonselectively with two electron donors L to give a second intermediate $Ru_3(CO)_{12}L$ (I'), the precursor to the photofragmentation products. Kinetic flash photolysis experiments were successful in demonstrating the presence of the latter type of intermediate for L = $P(OCH_3)_3$, PPh_3, cyclohexene, and THF. For the first two of these ligands, I' decays largely by fragmentation while loss of L to regenerate starting material is predominant for THF and cyclohexene. The fragmentation rates for I' can be qualitatively correlated with the π-acceptor σ-donor properties of L, the faster rates being observed for the stronger π-acceptors/weaker σ-donors.

The photosubstitution pathway is proposed to proceed by dissociation of CO to give the intermediate $Ru_3(CO)_{11}$ (II). Flash photolysis experiments in THF demonstrate the existence of a transient species, probably the THF adduct $Ru_3(CO)_{11}S$. Analyses of quantitative data from both CW quantum yield and kinetic flash photolysis studies lead to the conclusion that II is significantly more selective than is I toward reactions with ligands. For example, the reaction of II with CO is about eight times faster than with PPh_3. The greater selectivity of II is suggested to be a

consequence of this intermediate's ability to delocalize the unsaturation.

Acknowledgment. This work was supported by the National Science Foundation. Ruthenium used in these studies was provided on loan by Johnson Matthey, Inc.

Registry No. $Ru_3(CO)_{12}$, 15243-33-1; $Ru_3(CO)_{11}(P(OCH_3)_3)$, 82532-25-0; $Ru_3(CO)_{10}(P(OCH_3)_3)_2$, 78168-08-8; $Ru_3(CO)_9(P(OCH_3)_3)_3$, 38686-18-9; $Ru_3(CO)_{11}(P(p\text{-tolyl})_3)$, 83343-69-5; $Ru_3(CO)_{10}(P(p\text{-tolyl})_3)_2$, 100898-68-8; $Ru_3(CO)_9(P(p\text{-tolyl})_3)_3$, 38686-54-3; $Ru_3(CO)_{11}(P(o\text{-tolyl})_3)$, 86276-87-1; $Ru_3(CO)_{10}(P(o\text{-tolyl})_3)_2$, 100898-69-9; $Ru_3(CO)_9(P(o\text{-tolyl})_3)_3$, 100898-70-2; $Ru_3(CO)_{11}PPh_3$, 38686-52-1; $Ru_3(CO)_9(PPh_3)_3$, 15663-31-7; $Ru(CO)_5$, 16406-48-7; $Ru_2(CO)_6Cl_4$, 22594-69-0; $Ru(CO)_4(C_2H_4)$, 52621-15-5; $Ru(CO)_4(P(OCH_3)_3)$, 75641-93-9; $Ru(CO)_3(P(OCH_3)_3)_2$, 31541-94-3; $Ru(CO)_4PPh_3$, 21192-23-4; $Ru(CO)_3(PPh_3)_2$, 14741-36-7; THF, 109-99-9; 2-MeTHF, 96-47-9; CCl_4, 56-23-5; $P(OCH_3)_3$, 121-45-9; PPh_3, 603-35-0; $H_2C{=}CH_2$, 74-85-1; CO, 630-08-0; octane, 111-65-9; cyclohexane, 110-82-7; diglyme, 111-96-6; benzene, 71-43-2; pyridine, 110-86-1; acetonitrile, 75-05-8.

Four Zirconium Iodide Cluster Phases Centered by Boron, Aluminum, or Silicon

Jerome D. Smith and John D. Corbett*

Contribution from Ames Laboratory-DOE[1] and Department of Chemistry, Iowa State University, Ames, Iowa 50011. *Received October 4, 1985*

Abstract: Well-faceted crystals of $Zr_6I_{12}B$, $MZr_6I_{14}B$ (M = Cs or K), $Cs_{0.7}Zr_6I_{14}Al$, and $Cs_{0.3}Zr_6I_{14}Si$ are obtained in good yield from reactions of stoichiometric amounts of Zr, ZrI_4, CsI, or KI when appropriate and B, Si, or AlI_3 at 850 °C in sealed tantalum containers after 2 weeks. The compounds were established to be isostructural with $Zr_6I_{12}C$ (space group $R\bar{3}$) or $(Cs)Zr_6I_{14}C$ (*Cmca*), and one crystal structure for each of the four examples (M = Cs) was refined with use of single-crystal X-ray techniques. All of these compounds contain Zr_6I_{12}-type clusters with an interstitial B, Al, or Si (Z) atom in the center of the cluster at full occupancy. Changes in Z cause substantial changes in the host lattice, most directly in the size of the cluster where $\bar{d}$(Zr–Zr) ranges between 3.580 Å (Si) and 3.195 Å ($Zr_6I_{12}C$). The observed $\bar{d}$(Zr–Z) values are tenths of an angstrom less than those consistently observed in ZrZ_x phases, especially for aluminum. Extended-Hückel calculations illustrate the important role of the interstitial in providing both additional electrons and strong Zr–Z bonding to the cluster. Increasing Hi_i values for the interstitial valence orbitals in the order C, Si, B, Al reduce Zr–Z bonding and charge transfer to the interstitial atom, especially for aluminum 3p orbitals. The bonding in Zr_2Al shows some comparable properties.

In the past 3 years, the bonding of several light elements within metal cluster halides has been reported. The earlier examples pertained to carbon within condensed M_6X_{12}-type octahedral metal clusters of rare-earth and early transition metals where the cluster aggregation ranged from dimers through infinite chains and sheets.[2-8] Very recently, the bonding of several second-period elements—Be, B, C, N—within a variety of isolated $Zr_6Cl_{12}^{n-}$ clusters ($0 \le n \le 4$) has also been noted,[9] and the synthesis and characterization of three types of carbon-centered zirconium iodide clusters, $Zr_6I_{12}C$, $Zr_6I_{14}C$, and $MZr_6I_{14}C$ (M = K, Rb, or Cs), have been reported in detail.[10] Extended-Hückel calculations on the carbon-centered as well as on the hypothetical unoccupied iodide clusters of these types show that, as expected, the carbon 2s and carbon 2p orbitals interact strongly with molecular orbitals in the unoccupied clusters which are primarily zirconium 4d to stabilize the centered cluster via four rather low-lying Zr–C bonding orbitals. Four other Zr–Zr bonding orbitals are unchanged, so that a total of 14–16 electrons from the zirconium and carbon that remain after the iodine valence band is filled can be accommodated in these Zr–C and Zr–Zr bonding orbitals, as observed.

Zirconium iodide clusters appear to be particularly adaptable in accommodating other interstitial atoms, perhaps because of the larger halide and greater covalency of the bonding. One example occurs with the relatively large, centered potassium atom in the remarkable $Zr_6I_{14}K$.[11] Here somewhat different factors appear to be important in the bonding; the potassium 4p orbitals are now too high in energy to interact well with the apropriate Zr–Zr bonding orbitals, and interstitial bonding occurs mainly via the potassium 4s orbital. In compensation, however, additional Zr–I bonding results from improved Zr–I overlap when the zirconium octahedron expands to accommodate the larger interstitial and comes closer to the size of the cube defined by the 12 edge-bridging iodines.

These contrasting examples of interstitial bonding have led us to investigate whether other interstitial atoms might be included in the center of octahedral zirconium iodide clusters. Herein we report the synthesis, structural characterization, and the results of extended-Hückel calculations on four metal cluster halides containing three new interstitial atoms, boron in $Zr_6I_{12}B$ and $MZr_6I_{14}B$ (M = Cs or K), silicon in $Cs_{0.3}Zr_6I_{14}Si$, and aluminum in $Cs_{0.7}Zr_6I_{14}Al$.

Experimental Section

Materials. The purity, preparation, and handling of reactor grade Zr and ZrI_4 have been previously described.[12] Zirconium powder was prepared from metal strips through the formation and decompositon in

(1) Operated for the U. S. Department of Energy by Iowa State University under contract No. W-7405-Eng-82. This research was supported in part by the Office of Basic Energy Sciences, Materials Sciences Division.
(2) Warkentin, E. Masse, R.; Simon, A. *Z. Anorg. Allg. Chem.* **1982**, *491*, 323.
(3) Simon, A.; Warkentin, E. *Z. Anorg. Allg. Chem.* **1983**, *497*, 79.
(4) Schwanitz, U.; Simon, A. *Z. Naturforsch. B* **1985**, *40*, 710.
(5) Simon, A. *J. Solid State Chem.* **1985**, *57*, 2.
(6) Ford, J. E.; Corbett, J. D.; Hwu, S.-J. *Inorg. Chem.* **1983**, *22*, 2789.
(7) Hwu, S.-J.; Corbett, J. D.; Poeppelmeier, K. R. *J. Solid State Chem.* **1985**, *57*, 43.
(8) Hwu, S.-J.; Ziebarth, R. P.; Winbush, S. v.; Ford, J. E.; Corbett, J. D. *Inorg. Chem.*, accepted for publication.
(9) Ziebarth, R. P.; Corbett, J. D. *J. Am. Chem. Soc.* **1985**, *107*, 4571.
(10) Smith, J. D. Corbett, J. D. *J. Am. Chem. Soc.* **1985**, *107*, 5704.
(11) Smith, J. D.; Corbett, J. D. *J. Am. Chem. Soc.* **1984**, *106*, 4618.
(12) Guthrie, D. H.; Corbett, J. D. *J. Solid State* Chem. **1981**, *37*, 256.

0002-7863/86/1508-1927$01.50/0 © 1986 American Chemical Society